



Australian Government

Department of Agriculture, Fisheries and Forestry

# Technical Report

**Program and KPI:** Sub-program 1.3 KPI 1.19

**Report Title:** Refined design and deployment of a 3D imaging scanning rig in a beef abattoir

**Prepared by:** Dr Alen Alempijevic<sup>1</sup>, Dr Teresa Vidal Calleja<sup>1</sup>, Dr Raphael Falque<sup>2</sup>, Dr Malcolm McPhee<sup>2</sup>

<sup>1</sup>University of Technology Sydney and <sup>2</sup>NSW Department of Primary Industries

**Date published:** 30 January 2023



This project is supported by funding from the Australian Government Department of Agriculture, Fisheries and Forestry as part of its Rural R&D for Profit programme in partnership with Research & Development Corporations, Commercial Companies, State Departments & Universities.

## **Citation**

Alempijevic, A., Vidal Calleja, T., Falque, R., McPhee, M. (2023). Refined design and deployment of a 3D imaging scanning rig in a beef abattoir. *An Advanced measurement technologies for globally competitive Australian meat* Sub-program 1.1 KPI 1.19. January, No. 1. 23 pp

## **Acknowledgements**

This study was undertaken through the Advanced Livestock Measurement Technologies Project (ALMTech) and funded by the Department of Agriculture Rural Research and Development (R&D) for Profit program and Meat and Livestock Australia. Meat and Livestock Australia are thanked for their funding for data acquisition, and for access to commercial herds to compile the calibration datasets. The commercial partners JBS, TEYS and John Dee for their collaboration in generating this data.

## Abstract

This report details the steps in refining the 3D imaging scanning rig design to integrate into beef abattoir operations at chain speed. In order to provide early LMY estimation the rig was positioned at chiller entrance, acquiring hot carcass side 3D reconstructions as they leave the slaughter floor. The 3D digital shape of the carcass is analysed through a curvature descriptor that is associated to LMY values using a non-linear regression model. We posit that segmenting and identifying consistently correspondences between 3D carcasses allow for improved information gathered. Using 152 carcasses that have been 3D reconstructed and combining the curvature descriptor with HCW resulted in LMY estimation with RMSE 4.1% and  $R^2$  of 0.54, indicating that HCW provides independent observations to curvature, and assist in estimating LMY. The presented approach needs to be evaluated with more data to increase the confidence in estimated LMY and evaluating portability of model across different deployments.

## Executive Summary

Lean Meat Yield (LMY %) of carcass is an important industry trait, which currently is not routinely measured in Australian beef abattoirs. Objective on-line technology to determine LMY is key for wider adoption. This report presents the development, refinement and evaluation of a cost-effective, portable scanning rig based on RGB and depth cameras that can perform 3D reconstruction of hot carcasses in an abattoir at chain speed. The 3D digital shape of the carcass is analysed through a curvature descriptor that is associated to LMY values using a non-linear regression model. While the scanner could be positioned further down the processing chain, acquiring hot carcass sides at the chiller entrance has the potential to provide early LMY information that could be used to further optimise operations.

Identifying consistently the region in the 3D digital shape for LMY estimation is one of the key enablers of this development. . It allows systematic segmentation improving the information gathered and consistent extraction of features from 3D data, an essential precursor to formulating data-driven regression problems. We present improvements in our approach for surface correspondence and shape morphing of 3D carcasses. We validate the improvements of using consistent segmentation, and the of curvature rather than geometry such as volume to estimate LMY from 3D carcasses.

Using 152 carcasses that have been 3D reconstructed and combining the curvature descriptor with HCW resulted in LMY estimation with RMSE 4.1% and  $R^2$  of 0.54, indicating that HCW provides independent observations to curvature, and assist in estimating LMY. The presented approach needs to be evaluated with more data to increase the confidence in estimated LMY and evaluating portability of model to data acquired at different deployments. The opportunity to undertake this activity is forthcoming, with the 3D imaging scanner awaiting consolidated testing utilising a portable CT scanner as part of Programme 1 efforts in Q1 or Q2 of 2023.

# Contents

Citation .....	2
Acknowledgements .....	2
Abstract .....	3
Executive Summary .....	4
Contents .....	5
1 Introduction .....	6
2 Methods .....	7
2.1 Scanning Rig – Hardware Redesign .....	7
2.1.1 Initial 3D Scanning Rig System (2016 - 2018) .....	7
2.1.2 Improved 3D Scanning Rig System (2019 -) .....	8
2.2 3D Carcass Reconstruction .....	9
2.3 Consistent segmentation .....	10
2.4 Statistical Analysis .....	12
2.5 Dataset .....	14
3 Results .....	17
3.1 Evaluation of 3D Reconstruction Accuracy .....	17
3.2 Prediction of Lean Meat Yield .....	19
4 Discussion .....	20
5 Conclusions .....	21
6 References .....	22

# 1 Introduction

The overall objective of this work is the testing and validation of a low cost, portable, 3D Imaging Scanning rig as an objective technology for Lean Meat Yield of beef carcasses.

In order for the rig to operate at chain speed the first reported scanning process required modifications, enabled by alternative 3D cameras that Intel launched in mid-2018. Previous submitted reports have discussed the ability of the initial 3D scanning system, for reference please refer to; Report KPI 7.6.1 “3D imaging measurement of beef carcass composition, and analysis of improvement to 3D modelling”. We summarise the status of the system leading into the current KPI, the challenges present and modifications undertaken. Improvements to 3D reconstruction, and extraction of information used for modelling LMY from 3D shape as part of this process are investigated.

Changes in hardware and software needed to be validated with respect to 3D carcass reconstruction, as the 3D digital shape of the carcass is analysed through a curvature descriptor associated to LMY. We propose to validate the accuracy of 3D reconstructions against 3D shape acquired from medical CT, considered as ground truth. Repeatability testing of 3D reconstruction in-situ (at abattoir) needed to be performed.

We examine how the scanner will fit into standard abattoir operations, aiming at acquiring 3D information of hot carcass sides as they leave the slaughter floor. While the scanner could be positioned further down the processing chain, acquiring hot carcass sides at the chiller entrance could provide early LMY information that could be used to optimise product well ahead of progressing into the boning room.

Finally, with more acquisitions of 3D carcasses and portable CT acquired LMY, we anticipate portability testing to be undertaken, developing models of LMY estimation from one deployment, and validating this against others.

## 2 Methods

### 2.1 Scanning Rig – Hardware Redesign

#### 2.1.1 Initial 3D Scanning Rig System (2016 - 2018)

The first 3D scanning rig utilised 3D camera technology developed by Primesense at the core of the camera sensing system. These cameras revolutionised 3D acquisition, and were omnipresent in gaming consoles providing the state-of-the-art 3D capabilities. This sensor uses as operational principle structured light, which projects a known infrared (IR) pattern into the scene to recover depth information. However, the devices were not able to reliably resolve IR pattern ambiguity when using multiple emitters (cameras), which are a necessity to cover a large irregular shape such as a carcass, and would result in missing data when using overlapping camera field of views.

As a result, the initial beef carcass scanning rig needed by design to avoid overlap of camera field of views while still being able to acquire an entire beef carcass. This was achieved with a bespoke design with three vertical beams spaced 120 degrees apart, forming a circle around a rotating base wide enough to fit half a beef carcass or a full lamb carcass, as shown in Figure 1. Each vertical strut supports a rail and belt system on which a Primesense Carmine RGB-D sensor is mounted, such that it can move vertically. The spacing between the beams prevents the camera fields of view from overlapping.

To acquire the 3D shape of a carcass the rig was capable of rotating 360° with 5° increments, resulting in the cameras being able to not only move vertically, but also rotating around the carcass horizontally while facing the centre of the cylindrical shape. The structure therefore allows for the carcass to be placed in the centre of the rig, for scanning.

During scanning, the carcass, which is suspended in the abattoir chiller from a rail by the hind leg (suspended by the Achilles tendon), is manually moved along the rail into the centre of the rig; though this process would be automated in a production scenario. The cameras move up and down vertically as the base rotates 360° through discrete positions, acquiring a set of vertical strips of RGB-D images which cover the carcass from all angles other than from directly above and below. The motion of the rig is illustrated in Figure 1. To scan an entire carcass the rig moves cameras up (resulting in one “strip”), rotates 40°, moves cameras down (resulting in another “strip”). In total this results in 12 “strips” of the carcass with each camera covering 120° and the total coverage of the 3 cameras being 360°. A final 60° rotation allows the carcass to continue along the rail after scanning. The rig returns to original rotation, thereby integrating the scanning into the abattoir production process.

Testing of this rig was done in two abattoirs, JBS Brooklyn VIC 27 carcasses were scanned using a rig. The carcasses scanned were part of a larger study comprising 60 head of cattle evaluating the DEXA technology (Gardner, Peterse, Starling, Cook, Shirazi, & Williams 2017),, where the scanning activity was conducted over two consecutive weeks. A further 24 carcasses was collected using the rig at TEYS Wagga Wagga NSW over 2 days. Whole carcass side CT was not taken, rather LMY estimated from two primals. This dataset was not further utilised beyond testing the acquisition process.

Previous submitted report that discussed the initial 3D scanning system, for reference please refer to Report KPI 7.6.1 “3D imaging measurement of beef carcass composition, and analysis of improvement to 3D modelling” demonstrated the 3D models acquired could be used to estimate LMY%, RMSE was 4.34% and coefficient of determination  $R^2$  was 0.62. While the system is capable of handling a swinging carcass, in this preliminary study the acquisition time was in order of 3-5 minutes.

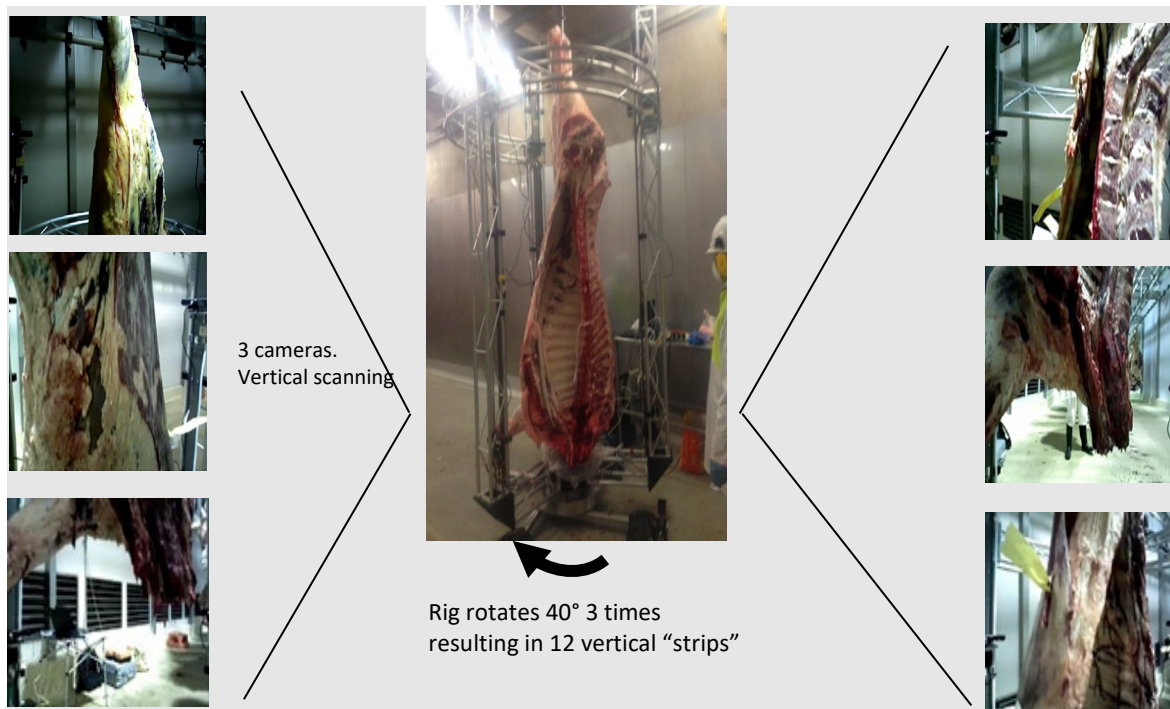


*Figure 1 – Initial scanning rig system deployed at NSW Abattoir in October 2016. The deployment did not have LMY estimated from CT, thus was not used to model LMY. Images on left and right are extracted from the 3D cameras during one up/down motion. The centre image shows the full rig and a carcass at the centre of the rig during scanning. The rig moves cameras up (resulting in one “strip”), rotates 40°, moves cameras down (resulting in another “strip”). This results in 12 “strips” of the carcass across 120°. The three cameras in total cover 360° around the carcass.*

### 2.1.2 Improved 3D Scanning Rig System (2019 -)

An iteration of the 3D scanning design was aimed at improving the time efficiency of scanning and ease of deployment. Crucial to time efficiency was removing constraints on the overlapping field of view, redundancy in 3D images a speed of 3D reconstruction.

Intel® started distributing a new range of depth (3D) cameras, Realsense D4XX range, in mid-2018. The operating principle in producing depth is based on IR assisted stereo reconstruction, thus overcomes issues with overlapping field of view between cameras.

Given the new cameras, instead of up/down motions of the 3 cameras followed by incremental motions a fixed installation of several cameras was possible. A single 360° sweep on the traverse of the carcass rather than its length could vastly improve acquisition time. A comparison of the two designs is depicted in Figure 2. The change in camera paths across the carcass would result in a reduced set of images that the reconstruction framework would need to process and a more constrained optimisation process to fully reconstruct the 3D

carcass. The mechanical design, software framework to support reconstruction and validation of the system in abattoir were the focus of work in fulfilling the KPI.

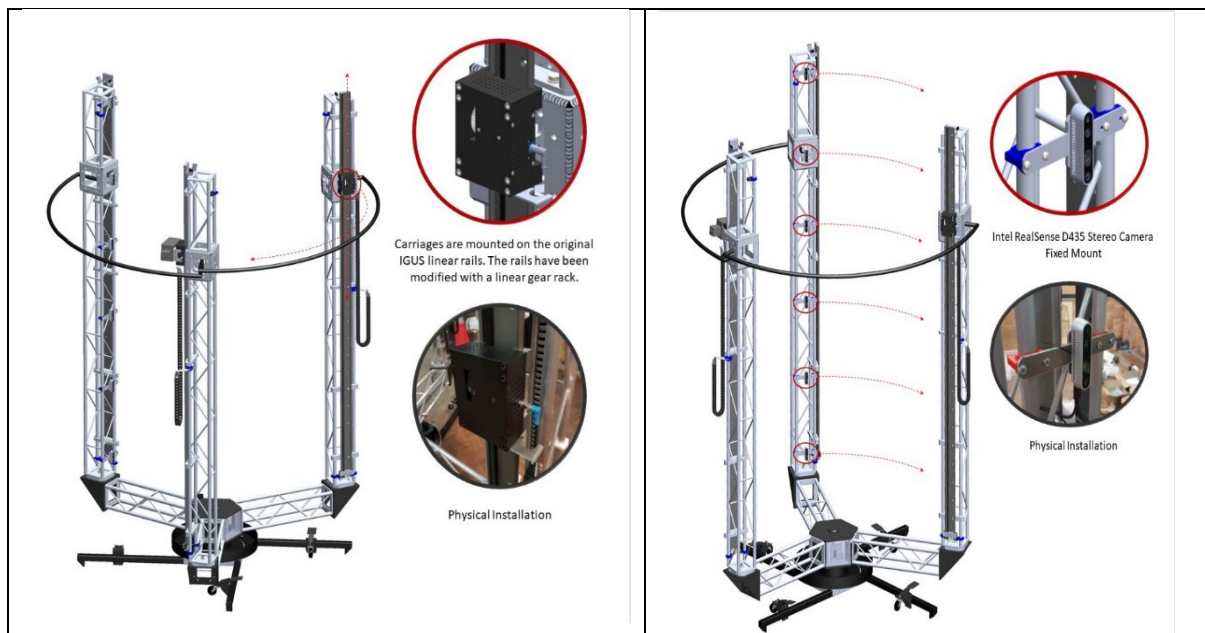


Figure 2 - Improvements of the 3D scanning rig design. Left: original design containing carriages that move the cameras up/down. Right: the design with fixed cameras on the horizontal beams, enabling 3D reconstruction of the carcass with a single sweep around the carcass.

## 2.2 3D Carcass Reconstruction

The method for 3D reconstruction used takes a series of colour (RGB) and depth (D) images as inputs, the pair is referred to as a frame, and generates a 3D pointcloud of a carcass. Parts of the image corresponding to the carcass are extracted from the background through simple geometric segmentation. Then, visual features with depth information are extracted to recover a subset of 3D points on the carcass. Correspondences between pairs of 3D points are found through image descriptors. These correspondences are used to find the relative transformation between frames. Given the relative transformations of the consecutive frames and across cameras, an optimisation algorithm (Kummerle, Grisetti, Strasdat, Konolige & Burgard, 2011) is used to obtain the best cameras trajectories (i.e., position and orientation of all cameras over time). A 3D reconstructed pointcloud can then be generated from the raw RGB-D data associated with each frame. Finally, a Poisson mesh reconstruction (Kazhdan & Hoppe, 2013) is run over the reconstructed pointcloud to create a closed surface mesh. Figure 4 shows a few sample reconstructed models.

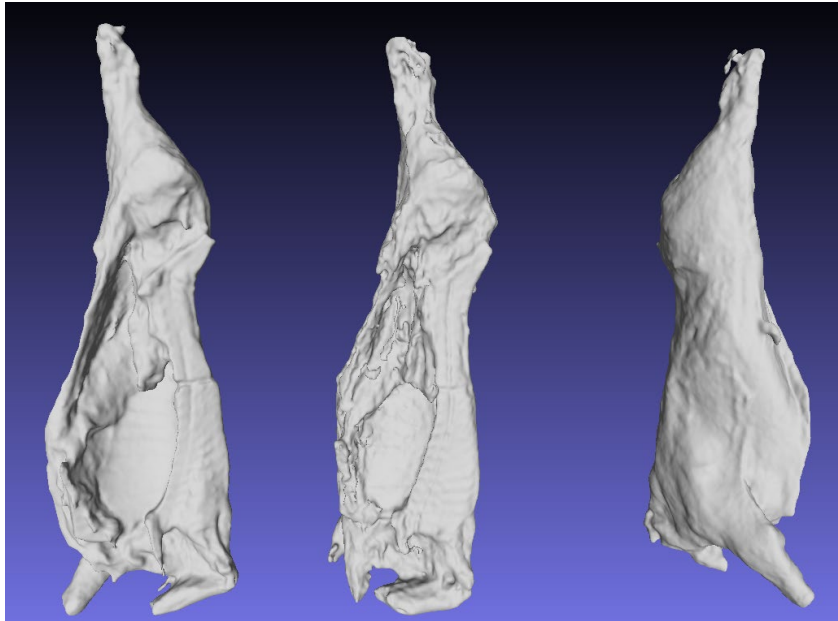


Figure 3 - Reconstructed 3D models of a beef carcass side

### 2.3 Consistent segmentation

In prior work on VIA technology (Rius-Vilarrasa, Bungler, Maltin, Matthews, & Roehe, 2009), the shape of the primal has been correlated with overall carcass LMY. The Europe SMY (Allen, 2009) also utilises a score assigned to the hindquarter shape (also known as “butt score”).

Key to the process, the region of the 3D shape where the descriptor used as an input of the LMY machine learning algorithm needs to be extracted consistently across all carcasses is the LMY, especially if focusing on muscle groups that belong to a specific area (such as a hindquarter). For example, a region of interest is shown in red in Figure 4.

In our approach, the consistency problem is solved by annotating the regions in one of the scanned 3D shapes, referred to as the annotated template of a carcass, and morphing this 3D shape in all the other 3D scanned carcasses, referred to as targets to segment the region of interest. The shape morphing is formulated as an optimisation problem obtained by solving the shape correspondence between the template and the target. The shape correspondence gives a function that maps the vertices of a shape to the vertices of another shape as shown in Figure 6. We use this map function to transfer the surface annotation from one shape to another. The annotations are then used to extract an area where the curvature descriptors are computed.

The shape correspondence method aims to achieve a consistent segmentation of the region of interest. The proposed method employs a coarse-to-fine approach (Falque, Vidal-Calleja, McPhee, Toohey, & Alempijevic, 2021). We developed a semi-automatic method where the coarse alignment is provided using manual annotations while the refinement step is performed automatically. We also implemented a fully automated approach that optimises the shape correspondence of a set of carcasses simultaneously, as shown in Figure 5, where all the constraints between each carcass are visualised as an edge of a graph.

Once the annotated template is finely aligned with the target, the annotation is transferred onto the target. Given this process for all carcasses, a curvature descriptor that is used for

estimation of LMY can be consistently obtained over the segmented region of interest. An example of the consistent segmentation is shown in Figure 6.

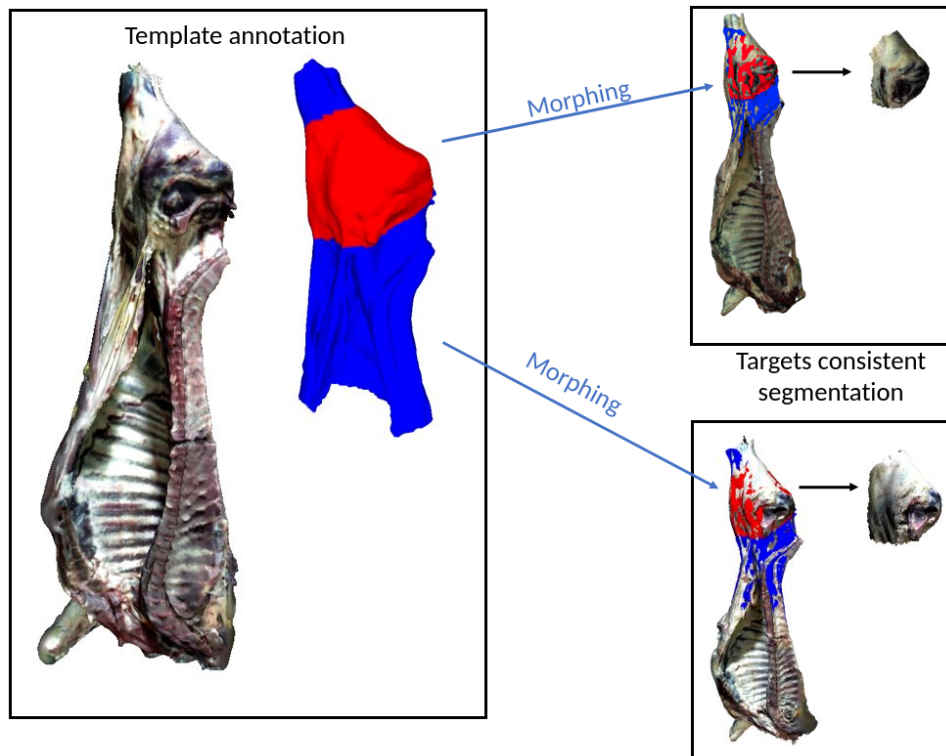


Figure 4 - Illustration of the consistent segmentation procedure. A template is carefully annotated to select a specific area of the carcass. This template is then morphed into all the other carcasses (i.e., targets) and the annotation is then used to extract the region of interest consistently across all the dataset.

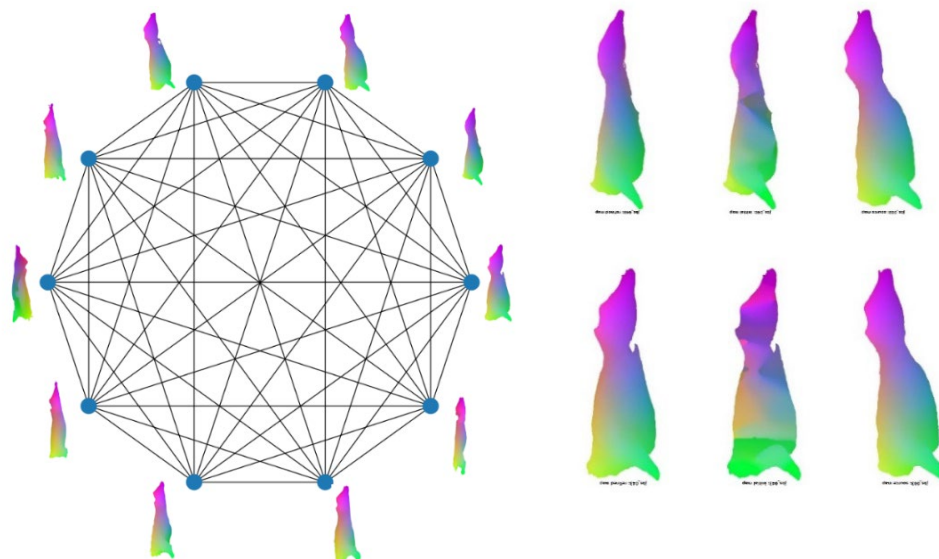


Figure 5 - The optimization method for solving the shape correspondence provides a function that maps the vertices of a carcass side to the vertices of any other carcass side. The colour indicates correspondence of parts of each carcass side.

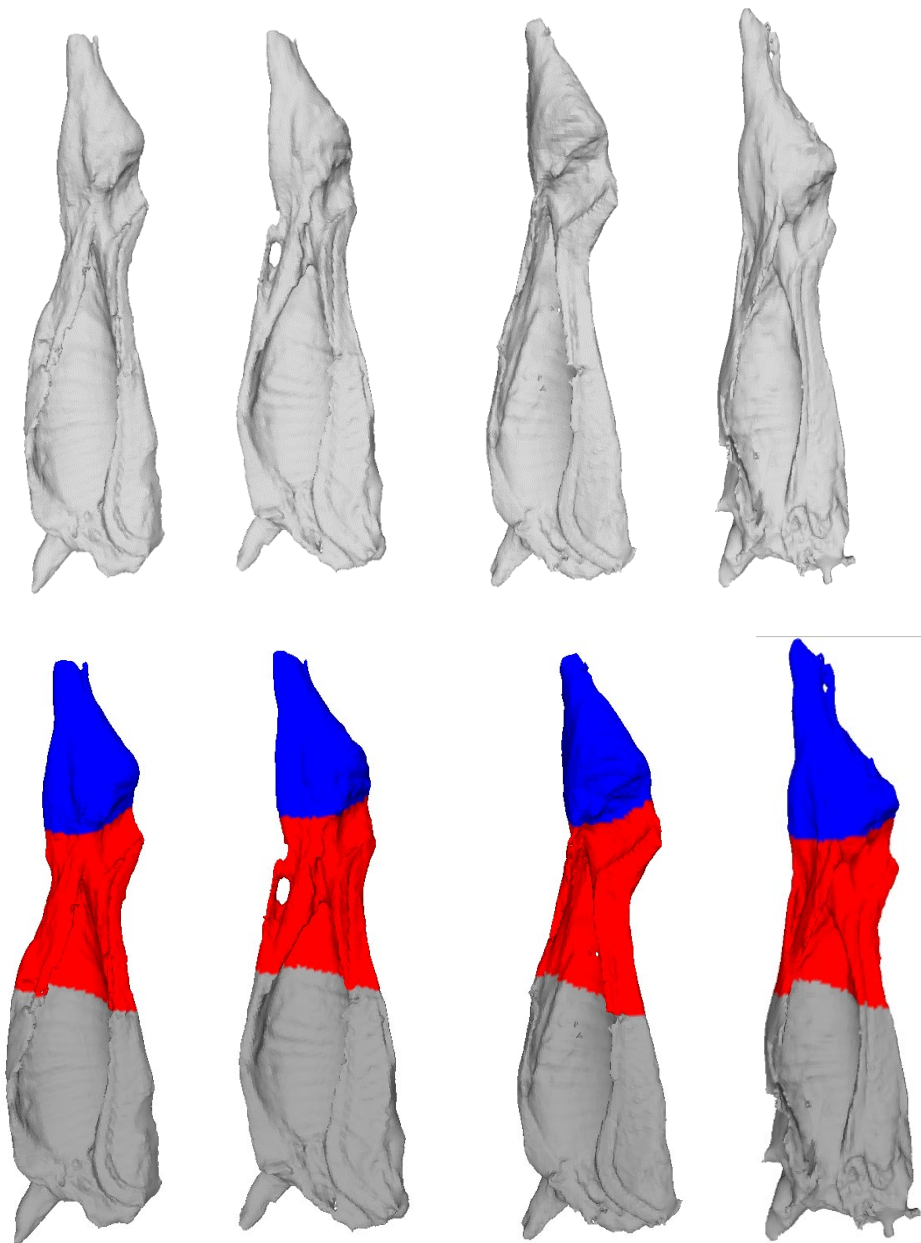


Figure 6 – Consistent segmentation of two regions across a number of carcasses sides. Top: reconstructions of 4 carcass sides. Bottom: annotations applied to the carcass's sides where the hindleg is annotated in red and hindquarter is red & blue collectively

## 2.4 Statistical Analysis

Gaussian Process (GP) model (Rasmussen & Williams, 2006) is a widely used approach for non-linear probabilistic regression. Given a set of training examples with ground truth information, a mean function, and a kernel function, this model aims to find the distribution that best fits the training set using maximum likelihood estimation.

A GP model, with a zero-mean function and a Matern kernel (Rasmussen & Williams, 2006), was trained in a supervised manner using  $h$ , the curvature descriptor, and optionally other

independent variables such as HCW or P8, and the ground truth of LMY as output. One of the important characteristics of GPs is the ability to provide a confidence value associated to the prediction, in the case of LMY.

GP regression is used with features based on the description of the shape curvature. Further details on curvature description are provided in (Alempijevic, Vidal-Calleja, Falque, Quin, Toohey, Walmsley, & McPhee, 2021).

All datasets were combined, and split into 85% training, 15% testing (10-fold cross validation). Given the trained GP regression model, new (previously unseen) carcass LMY can be estimated by inputting a carcass's curvature descriptor to the GP model.

## 2.5 Dataset

The evaluation of 3D Estimated LMY% was conducted using 152 carcasses of cows, steers, and heifers across a range of breeds at 2 abattoirs, where collection at abattoir A was undertaken on two occasions, annotated as A and A(2). The range of P8, EMA, HCW, and LMY for the dataset and from each abattoir is provided as histograms in Figure 7. Carcasses at all abattoirs averaged 2.5 meters in length and were all scanned within 30mins to 20 hours post-mortem. At abattoir A in first collection: 92 carcasses were scanned as part of 3 kills (separated by several months) by an operator using a hand-held prototype device and open-source software (Newcombe, Izadi, Hilliges, Kim, Davison, Kohli, Shotton, Hodges, & Fitzgibbon, 2011). At abattoir B 27 carcasses were scanned using a rig as outlined in 2.1.1. The carcasses scanned at abattoir B were part of a larger study comprising 60 head of cattle evaluating the DEXA technology (Gardner, Peterse, Starling, Cook, Shirazi, & Williams 2017), where the scanning activity was conducted over two consecutive weeks. Finally, at abattoir A in 2<sup>nd</sup> collection A(2): 33 carcasses were scanned using a rig as outlined in 2.1.2.

*Table 1 – 3D Imaging carcass acquisition statistics. The 3D scanning rig was deployed last two acquisitions, with the final design at the centre of the KPI and documented in this report deployed in June 2021*

Kill Date	Carcass Data Statistics			Location
	Available	Scanned	3D Reconstructed	
Nov 2013	31	31	31	Abattoir A
Feb 2014	31	31	31	Abattoir A
May 2014	31	31	31	Abattoir A
Oct 2016	51	47	26	Abattoir B
Jun 2021	32	32	32	Abattoir A(2)
TOTAL	172	168	151	

### Abattoir A:

The left-hand side of each carcass was processed with fat trimming limited to only that required for hygiene purposes and kidney fat was not removed. A MSA trade development officer using MSA protocols (Watson, Gee, Polkinghorne, Porter, 2008) graded all carcasses. After grading the left-hand side of the carcass was boned-out to determine beef primal cuts, fat trim and bone (Perry et al., 2001). The CT scanned lean and fat tissue weights were adjusted to untrimmed boneless primal weights. Recovery of boned-out components for 2 deployments were (n = 93) 99.3 0.58% and (n = 32) 98.3 0.19% (mean s.d.) of cold side weights, respectively.

### Abattoir B:

All carcass quarters were conventionally chilled for a further 24 hours before being processed into smaller pieces for CT scanning. The cold weight of each quarter was measured shortly after their removal from the chiller. Forequarters were cut into 9 smaller primal sections while hindquarters were cut into 7 sections. Each beef carcass was therefore CT scanned in a total of 32 sections, allowing all components to fit within the 500mm x 500mm CT aperture. The cutting lines used to cut each side into 16 sections were based on the abattoir cutting lines to enable subsequent dissection into saleable cuts of meat. The two sides of each carcass (spray-chilled and non-spray chilled sections) were CT scanned consecutively.

### **Computed Tomography:**

CT scanned data was captured using Picker PQ 5000 spiral CT scanners at either Murdoch University or the University of New England. In both cases the spiral abdomen protocol was selected with settings: pilot scan length of 512 mm, field of view set at 480mm, Index 20, kV 110, mA 150, revs 40, pitch 1.5 and standard algorithm. Prior to scanning the carcasses were dissected into 16 primal sections to t the limitations of the CT aperture. The primals were scanned in 10 mm or 5mm slice widths, with each slice taken 10 mm or 15mm apart. Image analysis was done according to the method described by Anderson et al., (2015).

Combined data resulted in a wide range of HCW and LMY values. The distribution of LMY (for the carcass side) over the entire dataset is denoted in Figure 7. Animals from abattoir B were on feed from 97 and 134 days prior to slaughter. As a result, the distribution of these animals, while covering a wider range, do not have a large overlap with the ones from abattoir A.

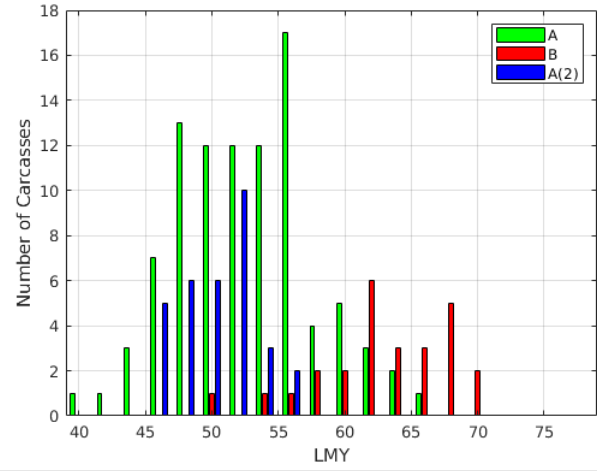
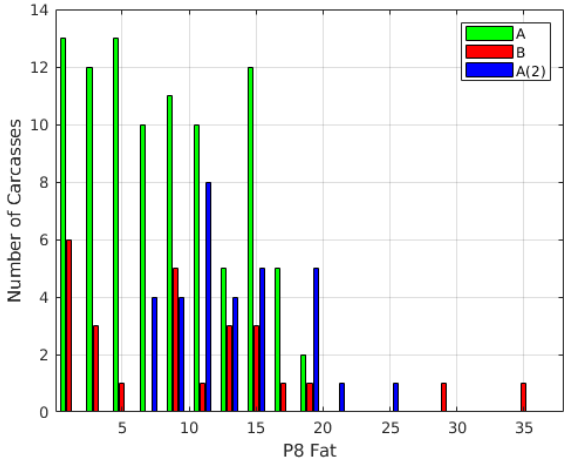
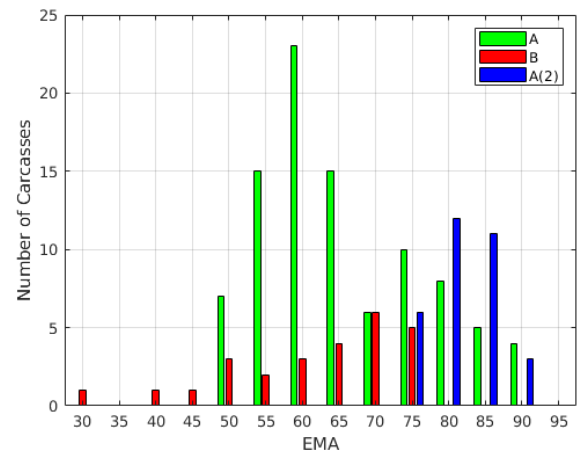
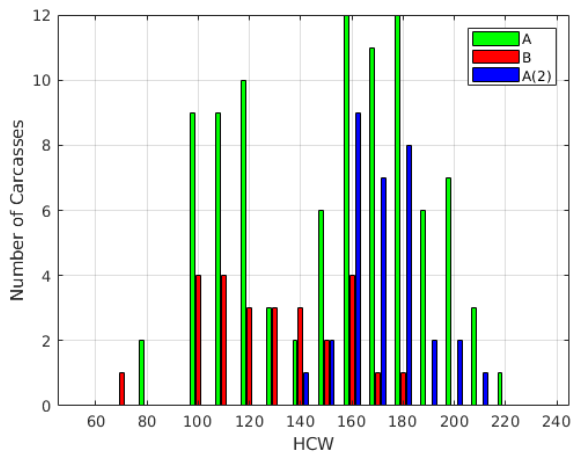


Figure 7 - Histograms of HCW, EMA, P8 and LMY for the 152 carcasses used in this report. The histograms are divided per abattoir deployment, green: Abattoir A, red: Abattoir B, and blue: Abattoir A (2<sup>nd</sup> deployment). The difference in distribution of objective traits is evident, the last deployment A2 are cattle that have been grain finished and a typical commercial feedlot output.

## 3 Results

### 3.1 Evaluation of 3D Reconstruction Accuracy

Given mechanical redesign and changes to the camera path when acquiring data an evaluation on the 3D scanning rig redesign was also undertaken in terms of speed, accuracy and repeatability of reconstruction. This was conducted in three phases

- 1) in house experiments on a fiducial (object the volumetric size of a carcass)
- 2) experiments on a carcass quarter (hindleg) undertaken at chillers of NSWPI
- 3) experiments repeating reconstruction on a carcass side in abattoir

In house tests confirmed scanning time for rig could be reduced to under a minute without any changes in reconstruction quality with information of the relative position between cameras. As these do not change after assembly of the rig the process of relative position computation was automated and enabled to be executed after assembly, at installation in chiller.

Phase 2 evaluate accuracy of 3D models, a carcass quarter (hind) was scanned at UNE chillers by both the 3D rig and CT scanner (the entire quarter was scanned). The CT information was used to reconstruct a CT 3D image. Comparing the two 3D reconstructions resulted in surface alignment with 99% of points within 2cm.

There is some non-rigid deformation of the beef quarter (due to it being laid on a CT bed, instead of hanging when it was scanned by our 3D carcass rig), which is evident in below images. Note that red areas are consistently above/below grey and not in patches on the image left and middle. This shows difference in appearance.

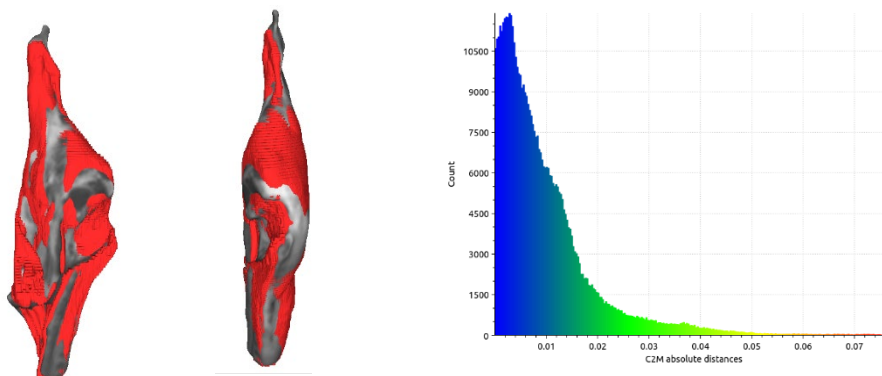


Figure 8 – Experiment on 3D imaging vs 3D CT reconstruction of a carcass quarter undertaken at UNE Armidale Chillers. Left: medial view Middle: dorsal view. In red is 3D camera reconstruction, grey is 3D CT reconstruction. Right: the point-wise cumulative distance between two surfaces (99% are within 2cm).

Small surface differences are expected as the carcass is transferred from being suspended to lying flat in a CT scanner. The relative volume difference was 4.26%. As a comparison, on 27 carcass sides acquired at Abattoir B (in 2016) using our previous 3D rig (CT scanned on-site) the mean volume error was marginally lower at 3.7%.

Phase 3 was postponed several times in 2020-2021 period due to NSW COVID restrictions. On borders opening to QLD in mid-2021 a trial on 32 carcass sides was organised at Abattoir A in QLD using cattle that are part of the NSW DPI Southern Cross Multibreed program.

We confirmed scanning time for rig at trial in June 2021 as 58s (load, scan, and release carcass side). The 3D reconstruction is possible in 30s (half the time). Exact scanning time would be contingent on the fidelity of the 3D carcass models where currently multiple images are used to reduce noise of final 3D reconstruction.

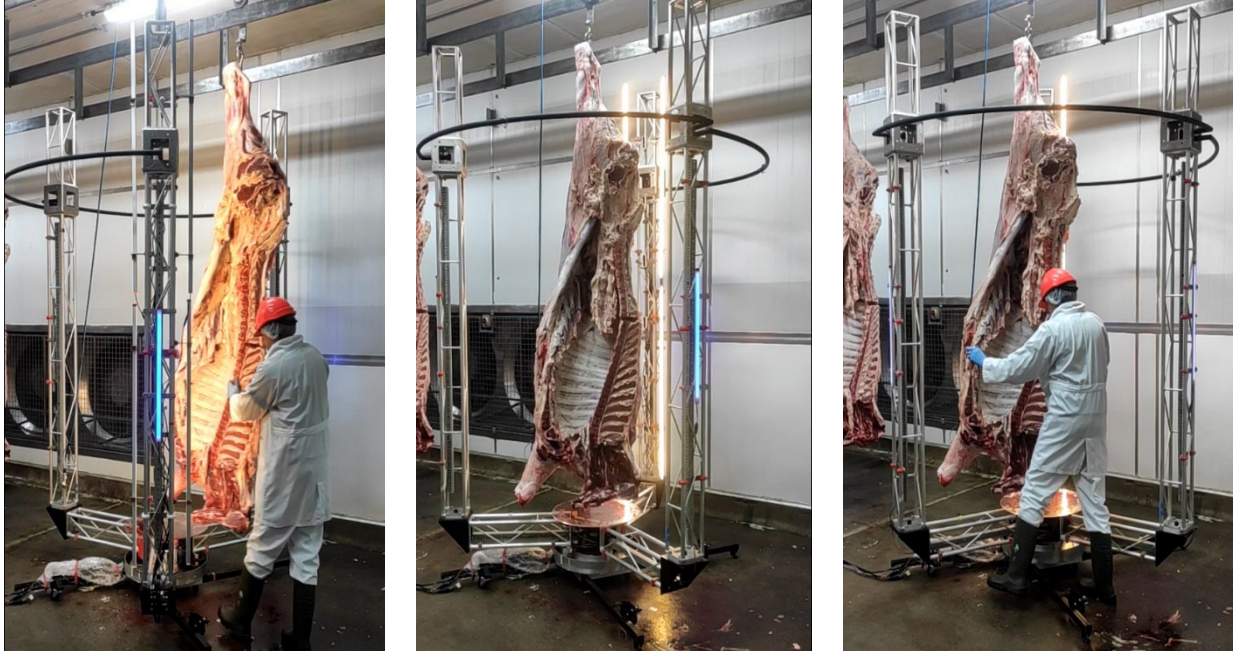


Figure 9 – Operation of 3D scanning rig at abattoir A (2<sup>nd</sup> data collection). Left: Carcass side is positioned in the rig, pushing it along the chain until it is approximately at the centre of the rig. Middle: The carcass is automatically scanned; the rig is in motion around the carcass. Right: The carcass is pushed out of the rig along the chain.

To investigate the repeatability of 3D reconstruction we scanned the same carcass in different orientations and with slight swing (carcasses are swaying on the rail at entrance to chiller). This resulted in identical 3D carcass models where 99% of the 3D carcass model are within 5mm, as demonstrated in Figure 4.

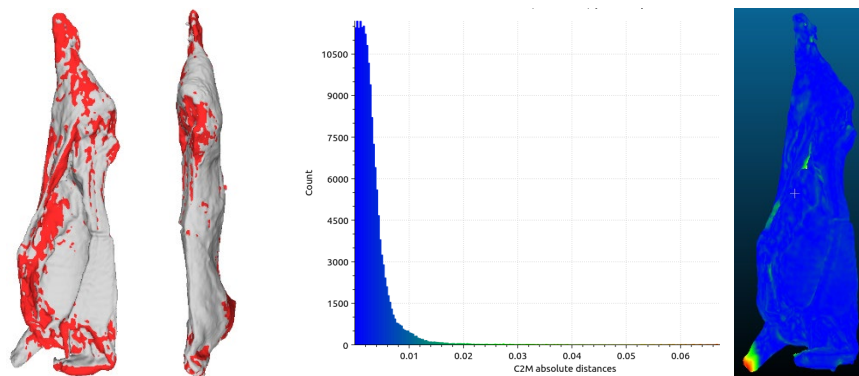


Figure 10 - Below images show: (a) medial and (b) dorsal view with - red scan 1 and grey scan 2 of same carcass, (c) is the point-wise cumulative distance between the two surfaces (99% are within 5mm) and (d) shows where the errors are (very top of foreleg was missing in one reconstruction).

Our further validation plans in 2021-2022 were affected by subsequent NSW COVID restrictions (started 24th June 2021) resulted in a few activities being postponed and needing to be rescheduled. The MLA - University of Sydney trial, which was to provide further carcasses to be scanned by the 3D scanning rig in the UNE chiller, was suspended due to COVID restrictions. The cattle for the trial were sold and a new trial date had not been established.

The 3D scanning rig was stored in Armidale NSW until November 2022 when it was shipped to Teys Rockhampton awaiting the consolidated trial for Programme 1 (including DEXA and E+V). We have been unable to further train independent staff (from NSW DPI) in use of the 3D scanning Rig, which is seen as a step forward towards commercial viability.

### 3.2 Prediction of Lean Meat Yield

We perform 10-fold cross-validation (using 85% of data for training a model and 15% for prediction, with the process repeated on 10 random folds. Utilising curvature and HCW in our model the LMY prediction has RMSE 4.1 and  $R^2$  0.54, detailed results presented in Figure 11).

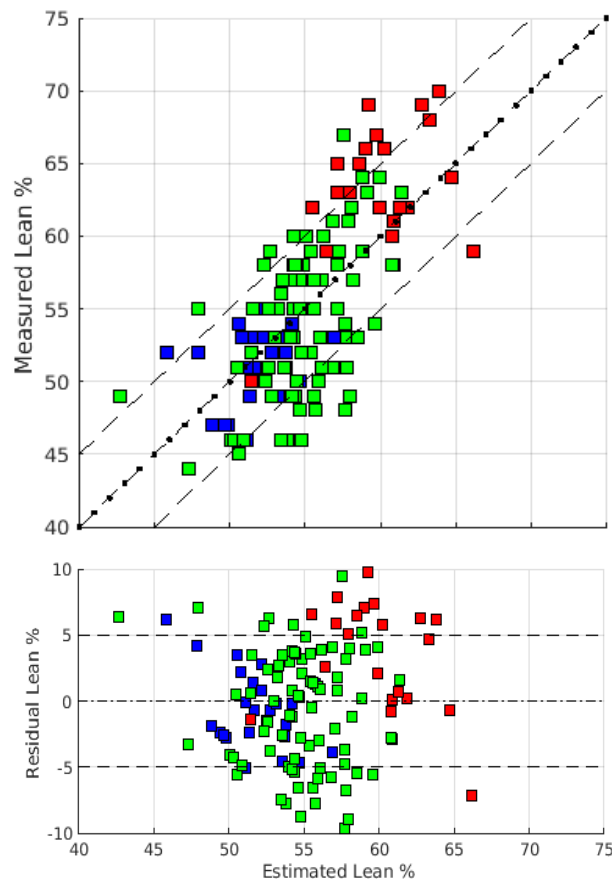


Figure 11 - Estimated LMY using 10-fold cross validation, colour coded are data from the three different data gatherings. Green: Abattoir A in 2013-14. Red: Abattoir B in 2016. Blue: Abattoir A in 2021 (noted as A(2)). Top: The Estimated vs Measured LMY, Bottom: Estimated LMY and associated estimation error compared to ground truth.

## 4 Discussion

The portable 3D scanning rig has been deployed in three beef abattoirs over the duration of the project, covering KPI 7.6.1 “3D imaging measurement of beef carcass composition, and analysis of improvement to 3D modelling” and the current KPI 1.19 “Refined design and deployment of a 3D imaging scanning rig in a beef abattoir”. The last deployment was at a beef abattoir where the rig was operating at chain speed while acquiring data of hot carcass sides.

The 3D scanning rig does not require any shielding, and was demonstrated to fit into standard abattoir operations. Carcasses sides were pushed into the chiller on the carcass rail from slaughter floor. They were scanned immediately on chiller entry before being stacked within the chiller. While the current scanning process required manual positioning of the carcass within the rig, there are no impediments to automate this process as 3D scanning and reconstruction was performed in chiller while the carcass was slowly swinging (only suspended by the hook on the rail).

During the three deployments, 3D data was acquired of hot carcasses at chiller entry, as well as carcasses 24h post mortem. Repeat scanning of a carcass side was also performed, the carcass was loaded and unloaded from the rig and scanned while it underwent some rotation and experienced motion of the foreleg. Scanning and 3D reconstruction was repeatable, analysis indicating 99% of the 3D carcass shape (points) were within 5mm.

We report LMY prediction on 151 carcasses using 10-fold cross validation has RMSE 4.1 and  $R^2$  0.54. The results are important for industry as an alternative low-cost solution for obtaining LMY estimation from hot carcasses on the slaughter floor, allowing to acquire information before chilling and subsequent processing.

Key to the consistent processing of 3D carcasses, where 3D information is used as an input of the LMY machine learning algorithm, is consistent extraction of regions across all carcasses. This is especially relevant when focusing on muscle groups that belong to a specific area and inform LMY, such as a hindquarter. Shape correspondence aims to achieve the consistent segmentation of the region of interest. We have developed and utilised a method which achieves high accuracy, employing a coarse-to-fine approach (Falque, Vidal-Calleja, McPhee, Toohey, & Alempijevic, 2021). Though our current methodology is computationally expensive, it can be implemented as real-time leveraging bootstrapping of sparse correspondence as per our work on 3D imaging in livestock (Falque, Vidal-Calleja & Alempijevic, 2023).

While 151 carcasses have been used to model LMY, only 58 were acquired with a 3D scanning rig. The data collected in 2013/14 at abattoir A was undertaken with a hand-held 3D scanner and generic 3D reconstruction code (Newcombe, Izadi, Hilliges, Kim, Davison, Kohli, Shotton, Hodges, & Fitzgibbon, 2011). Initial deployment of scanning rig at abattoir B in 2016 experienced technical difficulties with data logging and a mechanical failure in week 2. The last deployment, undertaken for this KPI, had 100% success in 3D carcass acquisition after vast improvements to the rig itself and software.

We have not yet been able to perform portability tests, training our model with LMY data from one abattoir and applying on the others. This is related to shear difference in LMY, HCW and

EMA across the different acquisitions. We are able to flag carcasses that are outside bounds of the current LMY model, this capability could be used to select carcasses that could be CT processed for ground truth. This information could be incorporated into the model and improve performance.

As the industry is looking towards calibration of devices that estimate LMY it is important to stress that acquisition of CT lean, used as gold standard in calibration, is a costly and complex endeavour. For devices using 3D information that do not penetrate the surface, such as ours, calibration between software or hardware upgrades is critical. In practise DEXA devices use fiducials (cubes of material) to assist calibration at one level of calibration, reducing need for CT data. We envisage it being possible to create 3D carcasses via 3D printing that facilitate calibration of devices that use camera technology. Using the “fiducial carcasses” calibration could be performed at the level of 3D reconstruction as well as extracting of features from shape that are used in learning. This would also reduce the amount of CT data needed in LMY calibration. Current 3D printing has not yet reached the volume of material needed, though we anticipate this to be possible in near future.

## 5 Conclusions

We conclude that the portable 3D scanning rig shows good potential for estimating LMY based on 3D reconstruction, curvature features and non-linear regression method, together with consistent segmentation of the region of interest. The deployment at a commercial abattoir, at chiller entrance was demonstrated to fit into standard abattoir operations of acquiring hot carcass traits. The scanner was positioned at chiller entrance, carcasses sides were pushed into the chiller from slaughter floor and scanned on entry before being stacked within the chiller. While current scanning process required manual positioning of the carcass within the rig, there are no impediments to automate this a process.

In total 151 carcasses had 3D shape acquired, covering a range of HCW, P8 EMA and corresponding CT evaluated LMY%. Curvature was extracted from the 3D models and combined with HCW, on the combined dataset 10-fold cross-validation was performed (using 85% of data for training a model and 15% for prediction, with the process repeated on 10 randomly drawn folds). The models resulted in prediction of LMY % with RMSE 4.1% and  $R^2$  0.54.

We have not yet been able to perform portability tests, training our model with LMY data from one abattoir and applying on the others. This is related to shear difference in LMY, HCW and EMA across acquisitions. The opportunity to undertake this activity is forthcoming, with the 3D imaging scanner awaiting consolidated testing utilising a portable CT scanner as part of Programme 1 efforts in Q1 or Q2 of 2023.

## 6 References

- Alempijevic, A., Vidal-Calleja, T., Falque, R., Quin, P., Toohey, E., Walmsley, B., & McPhee, M. (2021). Lean meat yield estimation using a prototype 3D imaging approach. *Meat science*, 181, 108470.
- Allen, P. (2009). 20 - Automated grading of beef carcasses. In J. P. K. Ledward, & David (Eds.), *Improving the Sensory and Nutritional Quality of Fresh Meat* (pp. 479-492). Woodhead Publishing.
- Falque, R., Vidal-Calleja, T., McPhee, M., Toohey, E., & Alempijevic, A. (2021). VirtualButcher: Coarse-to-fine Annotation Transfer of Cutting Lines on Noisy Point Cloud Reconstruction. In *2021 IEEE 21st International Symposium on Computational Intelligence and Informatics (CINTI)* (pp. 000109-000114). IEEE.
- Falque, R., Vidal-Calleja, T., & Alempijevic, A. (2023). Semantic keypoint extraction for scanned animals using multi-depth-camera systems. To be presented in *IEEE International Conference on Robotics and Automation (ICRA) IEEE*.
- Gardner, G., Peterse, J., Starling, S., Cook, J., Shirazi, M., & Williams, A. (2017). Developing a dual x-ray absorptiometer for estimating carcass fatness in beef at abattoir chain-speed. *International Conference on Meat Science and Technology*, (p. 722).
- Kazhdan, M., & Hoppe, H. (2013). Screened Poisson surface reconstruction. *ACM Transactions on Graphics (ToG)*, 32, 1-13.
- Kummerle, R., Grisetti, G., Strasdat, H., Konolige, K., & Burgard, W. (2011). g2o: A general framework for graph optimization. In *IEEE International Conference on Robotics and Automation (ICRA)* (pp. 3607-3613). IEEE.
- Newcombe, R. A., Izadi, S., Hilliges, O., Kim, D., Davison, A. J., Kohli, P., Shotton, J., Hodges, S., & Fitzgibbon, A. (2011). Kinectfusion: Real-time dense surface mapping and tracking. In *IEEE International Symposium on Mixed and Augmented Reality (ISMAR)* (pp. 127-136).
- Rasmussen, C. E., & Williams, C. K. (2006). *Gaussian processes for machine learning volume 1*. MIT press Cambridge.
- Rius-Vilarrasa, E., Bunger, L., Maltin, C., Matthews, K., & Roehe, R. (2009). Evaluation of video image analysis (via) technology to predict meat yield of sheep carcasses on-line under UK abattoir conditions. *Meat Science*, 82, 94-100.
- Watson, R., Gee, A., Polkinghorne, R., & Porter, M. (2008). Consumer assessment of eating quality-development of protocols for meat standards Australia (MSA) testing. *Australian Journal of Experimental Agriculture*, 48, 1360- 1367.